

## Proton-Induced Transient Effects in a Metal-Semiconductor-Metal (MSM) Photodetector for Optical-Based Data Transfer

C.J. Marshall<sup>1,2</sup>, *Member IEEE*, P.W. Marshall<sup>2,3</sup>, *Member IEEE*, M.A. Carts<sup>2,3</sup>, *Member IEEE*,  
R.A. Reed<sup>4</sup>, *Member IEEE*, K.A. LaBel<sup>4</sup>, *Member IEEE*

<sup>2</sup>NRL, Code 6611, 4555 Overlook Ave SW, Washington, DC 20375

<sup>3</sup>SFA, 1401 McCormick Dr., Largo, MD 20785

<sup>4</sup>NASA/GSFC, Code 562, Greenbelt, MD 20771

### Abstract

We present a study of proton transient effects in metal-semiconductor-metal (MSM) photodetectors, which demonstrates their inherent advantage for minimizing Single Event Effects (SEEs) in proton environments. Upset mechanisms are characterized for 830 nm GaAs and 1300 nm InGaAs detectors. Only protons incident at grazing angles are likely to cause a bit errors by direct ionization. The MSM technology appears to be a more robust to single bit errors than thicker 1300 nm p-i-n diode structures which we have previously shown to be susceptible to errors from direct ionization events at all angles, and also at relatively high optical powers [1].

For a given receiver, the relative contributions of direct ionization and nuclear reaction upset mechanisms at a specific data rate and optical power are determined by the geometry of the charge collection volume of the detector. We show that state-of-the-art p-i-n detectors can also display a reduced sensitivity to direct ionization by incident protons except at grazing angles.

### BACKGROUND

A substantial body of literature now exists which demonstrates the susceptibility of fiber-based data links to bit errors induced by transient events in the photodetector as a result of direct ionization by protons [1,2,3]. As with heavy ion single event effects, the geometry of the photodiode plays an important role, and there is an obvious advantage for relatively thin p-i-n structures fabricated using direct-bandgap materials (e.g. GaAs operating below 980 nm or InGaAs diodes from 980 to 1600 nm). The approximately 0.5-3  $\mu\text{m}$  thick p-i-n structures attainable using a direct bandgap semiconductor allow operation with excellent responsivity while minimizing the incident particle pathlengths in the detector charge collection region.

Motivation for this work follows from similar considerations for pathlengths in detectors fabricated using MSM structures. The diodes are formed with Schottky barrier junctions rather than p-i-n structures, and the resulting junction regions are usually substantially thinner (approximately 0.1-1  $\mu\text{m}$ .) The attractiveness of these structures

for optical communications follows from the low capacitance junction (formed by careful design of the interdigitated electrode structure) which allows high speed performance to many tens of gigabits per second [4-10]. Operation in the terahertz regime has been demonstrated using nanostructures [11]. The same small junction features should correspond to short particle pathlengths and relative improvements in bit error rate (BER) performance as compared to many commonly used p-i-n structures operated at the same wavelength and data rate, as a part of a comparable receiver design. Data shown here present results from the study of proton effects on of such devices.

In addition, we have examined the role of the direct ionization versus nuclear reactions as the mechanism responsible for particle-induced transients in MSM diodes. This has been accomplished by characterizing transient cross-sections produced by both heavy ions and protons at various energies as a function of the incident particle angle, and link optical power and data rate.

### INTRODUCTION

MSM photodetectors show promise for a variety of future optoelectronic data communications links, optical switching, chip interconnects, high-speed sampling systems, etc. Many variations of the MSM device structure exist, but they all employ two Schottky barriers with semiconductor in between. The electrodes are usually interdigitated to reduce capacitance, and the geometries are designed to optimize the electrical fields in the photo-carrier collection regions. Further improvements in material, design and lithography have resulted in vastly improved speed and frequency response for MSM diodes as compared to conventional diodes [4-10]. The ultimate operating frequency of an MSM diode may either be limited by the carrier transit time between the electrode fingers, or by the recombination time of the semiconductor material [12].

Despite the low quantum efficiency of most of these devices, their compatibility with planar field effect transistor (FET) technology is a key advantage to the development of high speed receiver systems. Techniques for improving the quantum efficiency are being investigated [13]. MSM diodes with lower dark currents (and hence better signal to noise behavior) have been developed using surface passivation techniques and improved device design [14]. The monolithic

<sup>1</sup> Currently employed in Code 562 at the NASA Goddard Space Flight Center, Greenbelt, MD 20771.

integration of the MSM with the pre-amplifier reduces the connection capacitance and amplifier noise to provide superior high frequency operation. MSMs are well established in integrated GaAs receivers, but monolithic Opto-Electronic Integrated Circuits (OEICs) using this technology are in the research or development stage for a variety of material systems. Discrete InP-based MSMs, and MSMs fabricated on low temperature grown GaAs are commercially available for multi-gigahertz operation. The MSM also has been integrated with the vertical cavity surface emitting laser (VCSEL) [15] which is a key enabling technology for high density optical communications.

### DEVICE DESCRIPTIONS

The two receivers studied are commercially available devices from Vitesse Semiconductor using their H-GaAs-III process. The target market for each device type is for Fiber Channel and Ethernet applications from 1.06 - 1.25 Gbps. Both receivers are packaged in a TO-46 header, and use a spherical ball lens to converge light onto the diode.

The GaAs MSM photodiodes (part number VCS7810) operate at  $\sim 830$  nm, and they are monolithically integrated with a TransImpedance Amplifier (TIA) and an Automatic Gain Control (AGC) circuit. The responsivity of the detector is  $\sim 35\%$ . It has a  $100\text{ }\mu\text{m}$  diameter with  $\sim 50\%$  of the area photosensitive, and a junction depth of about  $0.1\text{ }\mu\text{m}$  [16].

The VCS7810 receiver has two amplification stages and is fully differential. The front end is a TIA, and the output is essentially a buffer with a gain of two. In between the stages, there is a signal dependent restoring amplifier that adjusts the MSM bias (nominally at 3 V) so that under high current conditions, charge is bled off before it reaches the TIA [16].

We also characterized the Vitesse VCS7710 module that uses a very low capacitance  $1300\text{ nm}$  InGaAs p-i-n detector mounted directly to the same GaAs receiver circuitry described above. The fully depleted detector has  $<0.5\text{ pF}$  capacitance at the nominal operating bias of 3 V, but the effective capacitance in the circuit is not known. The p-i-n diode has an optically active diameter of  $75\text{ }\mu\text{m}$  and a responsivity of  $\sim 90\%$  [16]. It is manufactured by Telcom, Inc.

### EXPERIMENTAL

The device test set used in these studies has been described previously [1]. The key elements are a serial bit error rate test (BERT) set that generates a pseudorandom data sequence at 10 to 1100 Mbps used to modulate a solid state laser (an  $830\text{ nm}$  AlGaAs laser, or a  $1300\text{ nm}$  InGaAsP laser, depending on the particular diode under test). This optical signal passes through an attenuator, a lightwave power meter, and is then launched (via fiber) onto the photodiode under test. The diode output is amplified and fed back to the receiver side of the BERT for comparison with the original sequence. By logging the per cent of error free intervals, we verified that the particle-induced errors were caused by individual strikes. Cross section measurements were made with  $>100$  errors, except as noted.

Measurements were performed to assess proton bit error cross-section versus data rate, incident optical power, and angle of incidence. Data rates ranged from 100 Mbps to 1100 Mbps and optical powers were varied from  $-20.6$  to  $-5.5\text{ dBm}$  over the course of the tests.

The 63 MeV proton measurements were performed at the Crocker Nuclear Laboratory cyclotron located at the University of California at Davis. The dosimetry system has been described in previous publications [1] and is accurate to about 10%. Higher energy proton experiments were completed at the TRIUMF 500 MeV Proton Cyclotron Facility located at the University of British Columbia as described in [17]. Both ion chamber and plastic scintillator telescopes were used to measure the proton fluences, and the dosimetry is good to about 10%, except at the highest fluxes used ( $\sim 10^8\text{ cm}^{-2}\text{s}^{-1}$ ) for which the scintillators read about 15% low as a result of missed counts [18]. The heavy ion measurements were performed at the National Superconducting Cyclotron Laboratory (NSCL) located at Michigan State University. Dosimetry was performed using a real time parallel plate avalanche counter (PPAC) measurement for the carbon beam, and a surface barrier detector for the helium beam. In both cases, the measured fluences are expected to be accurate to within 30% [19].

### RESULTS AND DISCUSSION

Bit error cross-sections are evaluated as a function of incident proton energy, angle, data rate and optical power for two Vitesse receivers. Results of further experiments designed to elucidate the upset mechanisms and implications for on-orbit predictions are presented.

#### A. 840 nm GaAs MSM Receiver

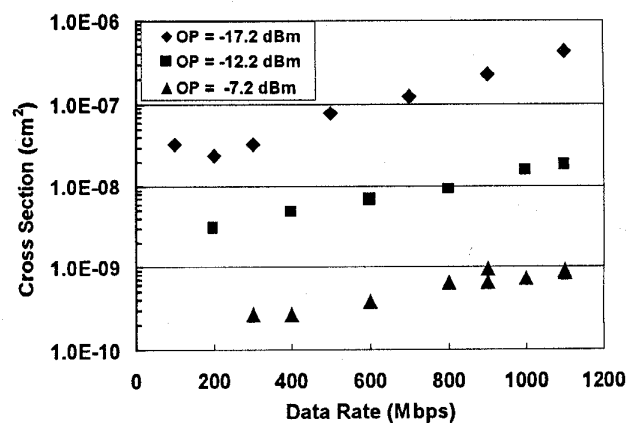


Figure 1. The BER cross-section dependence on data rate is most pronounced at an Optical Power (OP) of  $-17.2\text{ dBm}$  which is near the noise floor at the maximum data rate. These data correspond to a  $65^\circ$  angle of incidence.

Sample results of the data rate dependence are shown in the first figure which compares the data rate dependence of the cross-section at three optical power values for 63 MeV protons incident at  $65^\circ$  with respect to the normal to the plane of the photodiode. First note the approximately linear

dependence of the cross-section on data rate at -12.2 and -7.2 dBm, which provide link operation well above the noise floor. This behavior was previously observed in a p-i-n diode receiver by Marshall et al. [1], and investigated in detail for clocked logic by Reed et al. [20].

The receiver circuitry performs a "decision" on the clock edge associated with each bit period, and this represents the critical "decision time window" during which a transient can disrupt the data, as illustrated in figure 2. The time interval for this decision is set by the bandwidth and slew rates supported by the detection circuitry, and it is not dependent on the data rate at which the circuit is being operated. Hence, increasing the data rate proportionally increases the number of opportunities of bit errors, and the linear dependence is expected [1,20].

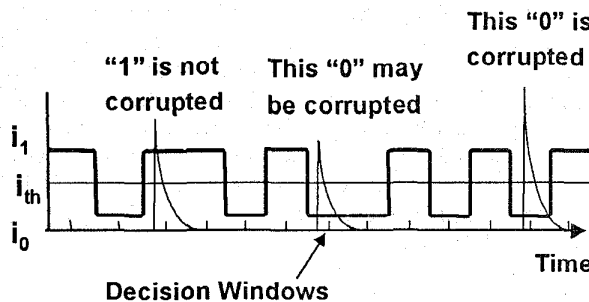


Figure 2. Pictorial of data stream of "ones" (current level,  $i_1$ ) and "zeroes" (current level,  $i_0$ ), and the threshold current level,  $i_{th}$ , for the "one state". The impact of several proton-induced transients is shown. (Decision windows are shown as points for clarity.)

The upper curve of figure 1 shows the data rate dependence of the link when operated at -17.2 dBm, which is the lowest operating power at the 1100 Mbps data rate. In this case, the bit error cross-section dependence on data rate is supralinear at -17.2 dBm. This illustrates how the link susceptibility to transient effects increases dramatically as conditions approach the noise floor at the maximum data rate and with minimum optical power.

The third figure illustrates the sharp dependence seen in the cross-section versus incident angle near  $90^\circ$  at which point the incident particle is parallel to the diode's plane. These data, corresponding to 400 Mbps operation at -12.2 dBm incident power (midrange for data rate and for optical power), show the  $>20\times$  increase in the bit error cross-section at  $90^\circ$ . This is taken to be evidence of the onset of the direct ionization mechanism for transient errors when long pathlengths traversing the thin dimension of the diode are possible. The magnitude of the error cross-section versus the diode size, and the absence of any angular dependence except at near grazing incidence, are taken to be evidence of the dominance of an indirect nuclear reaction-based mechanism at all other angles of incidence. We note that at  $65^\circ$ , the measured cross-section is about four orders of magnitude lower than expected based on the physical device area. This is consistent with an indirect mechanism since roughly one in  $10^4$  proton strikes would be expected to result in a nuclear reaction in the silicon detector for a 63 MeV proton.

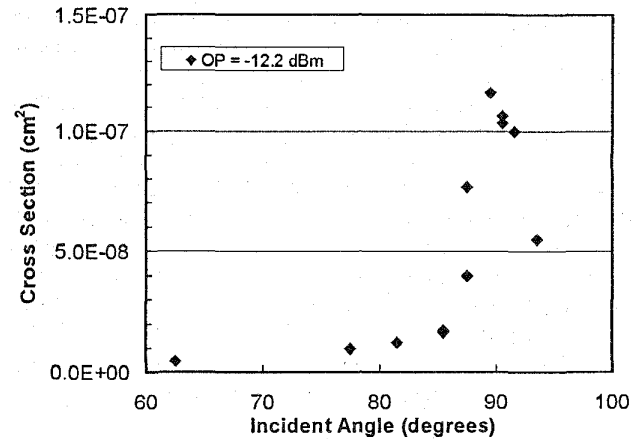


Figure 3. The bit error cross-section varies sharply with incident angle, but only close to  $90^\circ$ . These data correspond to 400 Mbps operation.

The two upset mechanisms are illustrated in figure 4. The pronounced angular dependence of the error cross-section was observed for incident proton energies from 68 – 491 MeV at the TRIUMF proton test facility. This underscores the importance of considering this phenomena in the prediction of on-orbit error rates.

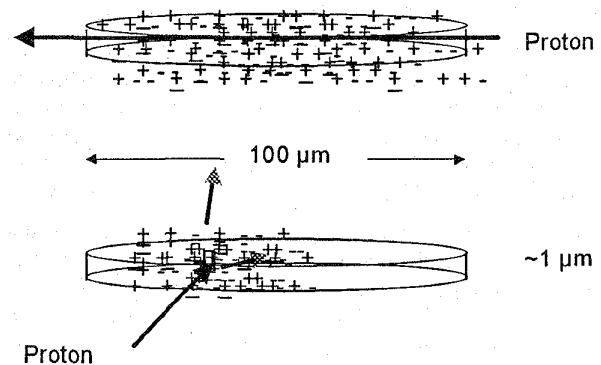


Figure 4. The upper picture illustrates the long pathlengths possible when a proton is incident at  $90^\circ$ . The lower diagram shows the dense ionization produced by the recoils generated in a nuclear reaction.

As discussed in [21], one would expect a significantly narrower angular distribution based on the very small acceptance angle about  $90^\circ$  required to traverse the length of the diode. We do not fully understand why the observed distribution is broader. However, as noted in [21], the incident proton beam has undergone multiple scattering in high Z foils before impinging on the device, and consequently has a distribution of trajectories. Some charge collection via diffusion may also occur leading to a smearing of the angular dependence. The possible contribution of nuclear elastic events to the angular spread is also being investigated [24].

To further investigate the proposed existence of two upset mechanisms, bit error measurements were performed using 240 MeV helium ions that produce carriers in the photodiode

solely via direct ionization. The helium error cross-sections are compared to proton cross-sections measured under identical operating conditions (400 Mbps, -12.2 dBm) in figure 5. The almost four order of magnitude increase in the helium cross-section at 65° provides clear support for the dominance of the indirect proton upset mechanism except at grazing incident angles where direct proton ionization becomes important. As an additional check, we verified that a heavily ionizing high atomic number ion (no nuclear reactions) would produce a bit error cross-section (near the noise floor of the receiver) comparable to the physical diode area. Indeed, the measured 400 Mbps bit error cross-section at 65° at 24 dBm with incident 740 MeV carbon ions, was within 30% of the physical detector area, as expected. The agreement was within the estimated experimental dosimetry uncertainty of ~30%.

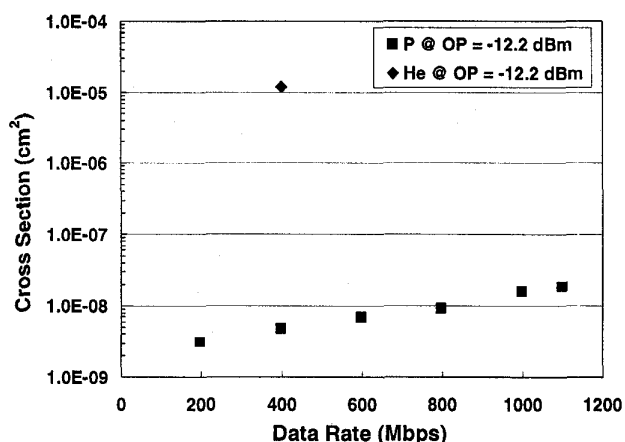


Figure 5. Error cross-section for incident helium and proton at 65° incidence. Most 63 MeV proton errors are attributed primarily to an indirect mechanism, whereas the 240 MeV helium errors are due exclusively to direct ionization.

A similar relation between cross-section and angle was described for the case of proton-induced optocoupler transients by LaBel, et al. [21]. The same arguments for direct ionization versus nuclear reaction-based transients presented in that work apply here. However, the sensitive angle range is considerably narrower in the present case, corresponding to a thinner geometry and diffusion volume as compared to the bipolar optocoupler technology studied to date [21,22,23]. The direct ionization upset mechanism would therefore be expected to play an even lesser role in an omnidirectional particle environment in space.

The relation between incidence angle and cross-section can be examined further with the help of figure 6. Here, the cross-sections at 400 Mbps operation are plotted versus optical power at incident angles of 65° and 90°. Note that the two curves converge at minimum optical power values. Between 21 and -15 dBm, the two curves diverge rapidly and then tend similarly with optical power up to the maximum value tested. Whereas the break from a constant power law relation is in the 90° data set, the 65° data follows a single power law dependence over the entire range of optical powers

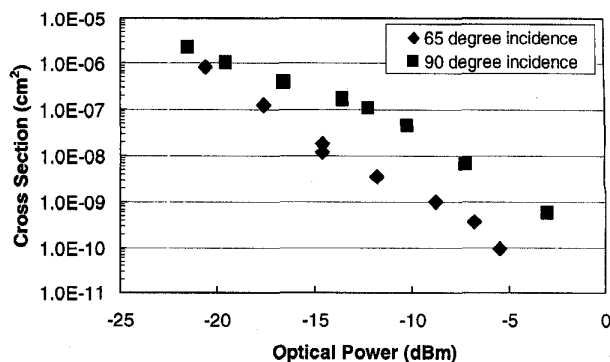


Figure 6. The error cross-section dependence on incident optical power is more pronounced with grazing incidence protons. The two curves meet at about -22 dBm but differ substantially at maximum incident power. These data correspond to 400 Mbps operation.

tested. Note further that the 90° data exhibits a maximum cross-section that is approximately identical to the physical area of the edge view of the planar disk (100  $\mu\text{m}$  diameter and about 0.5-1  $\mu\text{m}$  thick). This suggests that essentially all particles striking the diode at 90° incidence can disrupt data at the lowest optical power of -22 dBm. (There is a distribution of particle pathlengths through the detector for the 90° orientation, but uncertainties in the diode structure and incident angle do not allow this effect to be quantified.) The 65° curve never reaches the projected area of  $\sim 3.5\text{E-}05 \text{ cm}^2$  even at the lowest optical power, though it reaches a value orders of magnitude higher than expected based only on the indirect upset mechanism. It seems likely that both mechanisms are contributing to errors at the lowest optical power values.

Having noted these points, it is interesting to revisit the -17.2 dBm curve of figure 1. The cross-section in the top curve increases more rapidly (relative to the -12.2 and -7.2 dBm curves) with data rate. The combination of low power and maximum data rate do indeed approach the noise floor of the receiver, and it is likely that the -17.2 dBm data set is exhibiting the effects of the direct ionization mechanism as the data rate increases, even at 65° incidence.

An estimate of the LET threshold for bit upsets by direct ionization is possible using the proton angular dependence data in figure 3, and heavy ion measurements for which the only possible upset mechanism is direct ionization. Using figure 3, we can estimate that the direct ionization contribution to the bit upset cross-section turns on at approximately 86° which corresponds to an effective LET of  $0.098 \text{ MeV}\cdot\text{cm}^2/\text{mg}$  (corresponding to a critical charge of 2.2 fC). In the proton case, there is always some contribution from both the direct and indirect mechanisms so further measurements were performed using high energy helium ions. No bit upsets were observed with normally incident 240 MeV helium ions which provides a lower bound of  $0.064 \text{ MeV}\cdot\text{cm}^2/\text{mg}$  (corresponding to a critical charge of 1.5 fC) for the LET threshold at 400 Mbps and -12.2 dBm. Bit errors were observed with normally incident 720 MeV carbon ions, which provides an absolute upper bound of  $0.24 \text{ MeV}\cdot\text{cm}^2/\text{mg}$  (corresponding to a critical

charge of 5.9 fC) for the threshold LET. These values are consistent with the estimated critical charge for the receiver operation at -12.2 dBm and 400 Mbps. It is important to note that the critical charge is a function of the data rate and incident optical power on the detector.

### B. 1300 nm InGaAs p-i-n Receiver

For a given receiver, the existence of a relevant range of operating conditions for which both the direct and indirect proton interactions can cause bit errors is dependant on the detector geometry and charge collection characteristics. This combination of upset mechanisms has been observed in not only the GaAs MSMs, but also in a variety of optocouplers [21,22]. We also report here similar behavior in a very low capacitance InGaAs p-i-n diode with identical receiver circuitry as the 840 nm GaAs module described above.

The angular dependence of the cross-section versus optical power at 400 Mbps is characterized in figure 7. The angular variation is greatly reduced at both very low and very high optical powers. Close to the noise floor, most particle strikes result in a bit error since even relatively small events (e.g. direct ionization over short lengths) are sufficient to cause a bit error in the receiver. At high optical powers (sometimes used for point-to-point links), a nuclear reaction event that produces heavily ionizing recoil atoms is much more likely to produce a bit error. As a result, no angular dependence is observed.

Many optical data buses operate at the intermediate optical powers for which the angular dependence is significant, as seen in figure 7. At -17.5 dBm and 400 Mbps, we measure an order of magnitude difference in the bit error cross-section in going from 65° to 91°. The angular dependence should be considered when performing an on-orbit prediction.

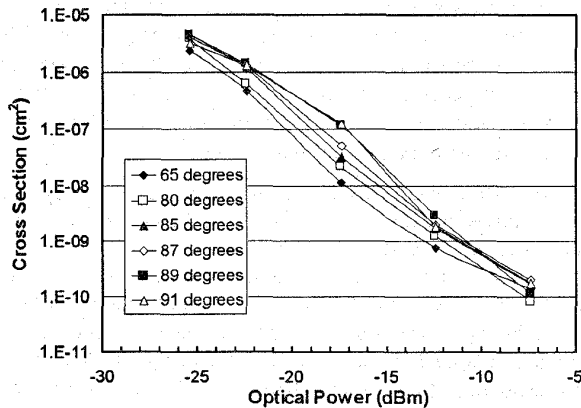


Figure 7. The angular dependence of the bit error cross-section (measured at 400 Mbps) varies significantly as a function of optical power.

### C. Space Prediction Issues

In order to perform an on-orbit prediction of a particular receiver's bit error rate, it is necessary to understand the upset mechanisms since they directly impact the model used to

predict the device performance. The transient radiation response of a receiver may not be obvious based on current understanding, and available detector and receiver circuitry information. In previous studies [1, and references therein], the 1300 nm p-i-n error cross-sections did not show the pronounced angular dependence observed here. The receiver circuitry in the earlier work is quite different than in the present study, and the diodes have different doping levels in their respective active volumes (and were operated with a different bias). For all these reasons, direct comparison of the results is not possible. Nevertheless, based on the limited information available, we might have expected a more similar transient response from the two 1300 nm receivers.

Another unexpected behavior is seen in the comparison of the optical power dependence of the bit error cross-sections in the high optical power regime for the two Vitesse receivers studied here. Given the fact that each detector exhibited a sensitivity to both upset mechanisms at intermediate optical powers, and the fact that the receiver circuitry is essentially identical for both the 840 nm and 1300 nm systems, we might have expected both modules to become significantly less sensitive to direct ionization events at high optical powers. This is the case for the 1300 nm module, but as can be seen from figure 6, the 840 nm receiver still has a significant angular dependence even at -5 dBm. Perhaps unknown differences in the respective detectors, their impedance matching to the GaAs receiver substrate and/or capacitance coupling issues are at the root of the variation in the transient response of the modules. Recall that only the 840 nm receiver is a monolithic device. It will take further investigation to resolve this issue.

Based on experiences such as the two described in this section, we believe it is premature for the community to make *a priori* judgements as to the degree to which a detector/receiver module will be susceptible to both the direct and indirect bit error mechanisms. Further charge collection studies and SPICE modeling of the receiver circuitry will be necessary to adequately characterize the transient response optically based receivers. Until a better understanding is acquired, it is essential to perform application-specific proton bit error testing to determine the cause of the upsets, so that the appropriate model can be used to make an on-orbit upset rate prediction enabling the technology to be evaluated for usage in space. The radiation testing should characterize the upset cross-sections as a function of incident particle energy and angle.

Once the appropriate ground-based transient testing has been performed, it will be necessary to calculate both the direct and indirect proton event rates in order to perform an on-orbit prediction of the bit error rate. Both contributions can be significant, and the bit error rate will depend on the receiver design, optical power (LET threshold), and diode geometry and charge collection characteristics. It will also depend on the particular proton energy spectrum as determined by the particular shielding configuration and orbit. As previously noted [21], it would be logical to develop a predictive method that combines the Bendel formalism for the proton direct reaction contribution to the bit error rate with the

modified Rectangular ParallelPiped (RPP) approach previously described by Marshall et al. [1] for direct ionization.

## CONCLUSIONS

Comparisons between the MSM-based detectors characterized in this work and the p-i-n diode-based structure examined here (and in [1]), illustrate fundamental differences in transient error mechanisms. For the case of the very thin MSM devices, the evidence suggests that nuclear reactions are required to initiate errors except at a quite narrow acceptance angle where protons can induce errors by traversing the long paths across the diode diameter. This claim is supported by the observed angular dependence, as well as the good agreement between our estimate of the critical charge at the apparent threshold for bit upsets produced by direct ionization at grazing angles. Further support for this hypothesis follows from the approximately four order of magnitude difference between proton and heavy ion cross-sections for non-grazing angles of incidence.

This work provides the basis for proceeding with the development of a bit error prediction model, which will be a complex task because of the existence of two mechanisms, and their relative importance which depends on a variety of factors including the environment, optical power, data rate, receiver circuitry, etc.

As was hoped, the MSM technology appears to be one of the more robust alternatives available for particle environments where BER effects are important. Previous studies on InGaAs p-i-n diode-based receivers showed that they were susceptible to errors from direct ionization events at all angles and also at relatively high optical power values [1]. In contrast, the current MSM structures appear to be susceptible only near grazing incidence. The expected on-orbit bit error rate performance should be dominated by nuclear reaction-based events except for operation at the very lowest possible optical powers (which is rarely a good idea). This suggests that MSM based receivers would result in order-of-magnitude reductions in orbital BERs as compared to many photodiode technologies since they typically employ very thin detector junctions.

The MSM detector investigated here operates at 840 nm, a wavelength which has been avoided in satellite hardware design efforts because of the inherently poor bit error response of Si-based detectors that require a relatively thick collection volume to obtain adequate responsivity. Yet, at 840 nm, the MSM solution offers several orders of magnitude reduction in uncorrected bit error rate as compared for example to the NASA SEDS 1 (SAMPEX) technology [1]. This is an important result since it is highly desirable for satellite designers to have the opportunity to utilize commercially available technology at a variety of wavelengths.

## ACKNOWLEDGMENTS

We appreciate support from the Defense Special Weapons Agency (DSWA) and NASA. The expertise of the accelerator personnel at the Crocker Nuclear Laboratory (University of California), TRIUMF (located at the University of British Columbia), and the National Superconducting Cyclotron Laboratory (Michigan State University) greatly facilitated this work. Graphics support from Martha O'Bryan is gratefully acknowledged.

## REFERENCES

- [1] P.W. Marshall, C.J. Dale, M.A. Carts, and K.A. LaBel, "Particle-Induced Bit Errors in High Performance Fiber Optic Data Links for Satellite Data Management," *IEEE Trans. Nucl. Sci.*, Vol. 41, pp. 1958-1965, Dec. 1994.
- [2] P.W. Marshall, C.J. Dale, and K.A. LaBel, "Space Radiation Effects in High Performance Fiber Optic Data Links for Satellite Data Management," *IEEE Trans. Nucl. Sci.*, Vol. 43, pp. 645-655, Dec. 1996.
- [3] K.A. LaBel, D.K. Hawkins, J.A. Cooley, C.M. Seidlick, P. Marshall, C. Dale, M.M. Gates, H.S. Kim, and E.G. Stassinopoulos, "Single event effect ground test results for a fiber optic data interconnect and associated electronics," *IEEE Trans. Nucl. Sci.*, Vol. 41, pp. 1999-2004, Dec. 1994.
- [4] S. Bishop, I. Adesida, J.J. Coleman, T.A. DeTemple, M. Feng, K. Hess, N. Holonyak, Jr., S.M. Kang, G.E. Stillman, and J.T. Verdeyen, "The Engineering Research Center for Compound Semiconductor Microelectronics," *Proceedings of the IEEE*, Vol. 81, No. 1, pp. 132-151, 1993.
- [5] E. John and M. B. Das, "Design and Performance Analysis of InP-Based High-Speed and High Sensitivity Optoelectronic Integrated Receivers," *IEEE Trans. El. Dev.*, Vol. 41, No. 2, pp. 162-170, 1994.
- [6] R. P. Joshi and J.A. McAdoo, "Picosecond dynamic response of nanoscale lot-temperature grown GaAs metal-semiconductor-metal photodetectors," *Appl. Phys. Lett.*, Vol. 68, No. 14, pp. 1972-1974, 1996.
- [7] B.J. Van Zeighbroeck, W. Patrick, J. Halbout, and P. Vettiger, "105-GHz Bandwidth Metal-Semiconductor-Metal Photodiode," *IEEE Electron Dev. Lett.*, Vol. 9, pp. 527-529, Oct. 1988.
- [8] L.F. Lester, K.C. Hwang, P. Ho, J. Mazurowski, J.M. Ballingall, J. Sutliff, S. Gupta, J. Whitaker, and S.L. Williamson, "Ultrafast, Long-Wavelength Photodetectors Fabricated on Low-Temperature InGaAs on GaAs," *IEEE Phot. Tech. Lett.*, Vol. 5, pp. 511-517, May 1993.
- [9] P. Fay, W. Wohlmuth, C. Caneau, and I. Adesida, "18.5 GHz Bandwidth Monolithic MSM/MODFET Photoreceiver for 1.55- $\mu$ m Wavelength Communication Systems," *IEEE Phot. Tech. Lett.*, Vol. 8, pp. 679-681, May 1996.
- [10] E.H. Botcher, E. Droge, D. Bimberg, A. Umbach, and H. Engel, "Ultra-Wide-Band (>40 GHz) Submicron InGaAs Metal-Semiconductor-Metal Photodetectors," *IEEE Phot. Tech. Lett.*, Vol. 8, pp. 1226-1228, Sep. 1996.

- [11] S.Y. Chou and M.Y. Liu, "Nanoscale Tera-Hertz Metal-Semiconductor-Metal Photodetectors," *IEEE J. Quant. Elect.*, Vol. 28, pp. 2358-2368, Oct. 1992.
- [12] W.C. Koscielniak, J. Pelouard, and M.A. Littlejohn, "Intrinsic and Extrinsic Response of GaAs Metal-Semiconductor-Metal Photodetectors," *IEEE Phot. Tech. Lett.*, Vol. 2, pp. 125-158, May 1990.
- [13] M. C. Hargis, S.E. Ralph, J. Woodall, D. McInturff, A.J. Negri, and P.O. Haugsjaa, "Temporal and Spectral Characteristics of Back-Illuminated InGaAs Metal-Semiconductor-Metal Photodetectors," *IEEE Phot. Tech. Lett.*, Vol. 8, pp. 110-112, Jan. 1996.
- [14] W.A. Wohlmuth, P. Fay, and I. Adesida, "Dark Current Suppression in GaAs Metal-Semiconductor-Metal Photodetectors," *IEEE Phot. Tech. Lett.*, Vol. 8, pp. 1061-1063, Aug. 1996.
- [15] Private communication with Mary Hibbs-Brenner of Honeywell Corporation.
- [16] Private communication with Ray Milano of Vitesse Corporation.
- [17] E.W. Blackmore, B. Evans, M. Mount, C. Duzenli, R. Ma, T. Picles, and K. Paton, "Operation of the TRIUMF Proton Therapy Facility," to be published in the *Proceedings of the 1997 Particle Accelerator Conference*, Vancouver, British Columbia, May 1997.
- [18] Private communication with Ewart Blackmore of TRIUMF.
- [19] Private communication with Terry Grimm of the National Superconducting Cyclotron Laboratory.
- [20] R.A. Reed, M.A. Carts, P.W. Marshall, C.J. Marshall, S. Buchner, M. LaMacchia, B. Mathes, and D. McMorow, "Single Event Upset Cross Sections at Various Data Rates," *IEEE Trans. Nucl. Sci.*, NS-43, No.6, pp. 2862-67, Dec. 1996.
- [21] K.A. LaBel, P.W. Marshall, C.J. Marshall, M. D'Ordine, M. Carts, G. Lum, H.S. Kim, C.M. Seidleck, T. Powell, R. Abbott, J. Barth, and E.G. Stassinopoulos, "Proton-Induced Transients in Optocouplers: In-Flight Anomalies, Ground Irradiation Test, Mitigation and Implications," *IEEE Trans. Nucl. Sci.*, NS-44, No. 6, pp. 1885-1892, Dec. 1997.
- [22] R.A. Reed, P.W. Marshall, A.H. Johnston, J.L. Barth, C.J. Marshall, K.A. LaBel, M. D'Ordine, H.A. Kim, and M.A. Carts, "Emerging Optocoupler Issues with Energetic Particle-Induced Transients and Radiation Degradation," to be published in *IEEE Trans Nucl. Sci.*, NS-45, No. 6, Dec 1998.
- [23] A.H. Johnston, G.M. Swift, T. Miyahira, and S. Guertin, "Single-Event Upset Effects in Optocouplers," presented at the 1998 Nuclear Space and Radiation Effects Conference, Newport Beach, CA, Jul. 1998.
- [24] P.J. McNulty, W.W. Savage, D.R. Roth, and C.C. Foster, "Possible Role for Secondary Particles in Proton-Induced Single Event Upsets of Modern Devices," presented at the 1998 Nuclear Space and Radiation Effects Conference, Newport Beach, CA, Jul. 1998.